Link to official URL (if available):

Estimation of Voltage-Driven Reinforcement Cost for LV Feeders under 3-Phase Imbalance

Kang Ma, Chenghong Gu, *Member, IEEE*, Furong Li, *Senior Member, IEEE*

Abstract—**Three-phase imbalance causes uneven voltage drops along low voltage (LV) feeders. Under long-term load growth, the phase with the lowest terminal voltage will trigger network reinforcements, which are earlier than if the three phases were balanced. This leads to a higher voltage-driven reinforcement cost (VRC) than the balanced case. Three-phase power flow analyses are not suitable for VRC estimations under serious data deficiency (without customers' phase connectivity and smart metering data), and are not scalable due to the iterative nature which brings a prohibitively high computation burden on a utility level with millions of feeders. To overcome the challenges, this paper proposes a novel scalable methodology for VRC estimations that is applicable from an individual feeder to millions of feeders where the level of information is insufficient to support accurate three-phase power flow studies. The key is to use five types of load current distributions to represent customers' phase allocations and individual demands, and to incorporate these distributions into an equivalent impedance matrix which allows a straightforward VRC estimation without iterations. This paper applies this methodology to an individual feeder, showing that: 1) the VRC decreases (increases) with the increase of the K (beta) factor of the trapezoid (triangular-rectangular) distribution, given that other conditions remain the same; 2) the VRC is more sensitive to voltage imbalance than to current imbalance; and 3) if the three phases are balanced, the change of any single variable results in an increase of the VRC, given that all other input variables remain constant.**

Index Terms—**power distribution, power system economics, three-phase electric power, low voltage network, network investment, three-phase imbalance**

I. INTRODUCTION

THREE-phase imbalance causes inefficient uses of low voltage (LV) network assets. An imbalanced allocation of single-phase loads in a three-phase LV network causes voltage and current imbalance [1-3] and uneven voltage drops along the feeder [4]. At the same time, a long-term load growth causes a long-term decrease of the terminal voltages in LV networks [4], the majority of which are neither monitored nor controlled [5, 6]. When long-term load growth is coupled with three-phase imbalance in passive LV networks, there will be a phase whose voltage drops to the statutory lower limit earlier than the other two phases, thus prompting the distribution network operator (DNO) to take actions – a common practice is network reinforcements [7], which bring a voltage-driven

reinforcement cost (VRC). There are two major challenges associated with the VRC estimation: 1) the lack of visibility along LV feeders, as is the general case over the UK DNO's service areas; and 2) VRC estimations at a utility level in future would require an efficient and scalable method, applicable from an individual feeder to millions of feeders. Three-phase power flow studies are capable of computing the VRC for individual feeders with full smart metering data, customers' phase allocation data, and location-dependent impedance. But they are not applicable when these data are absent; and applying them to millions of feeders means a prohibitively high computational burden due to i) the extensiveness of LV networks with varying characteristics across different regions; and ii) the iterative nature of power flow analyses. To address the challenges, this paper focuses on the development of a scalable methodology for VRC estimations under severe data deficiency.

Existing papers and reports on LV network reinforcement costs are mainly based on balanced three phases. Voltage constraints are a key driver for network reinforcements (especially for rural networks), of which the costs were quantified on a utility scale under balanced three phases [8]. Other references on LV network investments [9-11], LV network expansion planning [12, 13], and smart network planning strategies [14-16] all assumed balanced three phases. Reference [17] estimated the voltage drops under balanced three phases, considering three typical load current distributions.

LV networks experience non-trivial three-phase imbalance [3, 18]. Numerous publications focused on power losses resulting from three-phase voltage and current imbalance [19-21]. Furthermore, a number of publications focused on the impact of voltage imbalance on the customer side, e.g. customers' induction motors [22-24]. While power losses and potential damages to customers' appliances are both key issues from three-phase imbalance, the increased reinforcement costs are no less important. However, there is very limited work on LV network reinforcement costs considering three-phase imbalance. References [25, 26] mentioned the impact of three-phase imbalance on network reinforcements qualitatively. Reference [27] quantified additional reinforcement costs from three-phase imbalance, considering thermal constraints only. Our recent paper on the quantification of the VRC for a typical LV circuit [4], however, has the following limitations: 1) it was limited to a typical LV circuit as a combination of a transformer and a feeder where the neutral line current is zero for this specific combination; and 2) it assumed a uniform distribution of load currents.

Now this paper makes a fundamental upgrade to the methodology: we propose a novel scalable methodology

VRC estimations where the level of information required for an accurate three-phase power flow study is not available. The methodology effectively addresses the limitations of the previous work by incorporating the impact of the neutral current into an impedance matrix and considering more general distribution patterns of load currents. It consists of a novel general VRC model and five novel specific VRC models: five typical load current distributions (uniform, head-dominated triangular, tail-dominated triangular, trapezoid, and triangular-rectangular distributions) are incorporated into an equivalent impedance matrix which is invariant under demand growth, thus allowing for a non-iterative estimation of the VRC.

The proposed methodology allows DNOs to estimate VRCs under severe data deficiency – only substation-side voltages and currents are required. This is particularly useful in the UK where there is a lack of visibility along LV feeders [28]. Furthermore, it works not only for an individual feeder but is also scalable to a utility level because of its non-iterative analytical nature.

It should be noted that network reinforcements are a common practice for DNOs to address the voltage issues caused by the demand growth in imbalanced three-phase LV networks [7, 8]. Such a practice is not necessarily the least-cost solution. In future, with increasing knowledge of customers' phase connectivity, it is possible to adopt alternative solutions to address the voltage issues and defer network reinforcements, e.g. phase balancing [25], demand side managements, and energy storage [29, 30], and the use of static VAR compensator [31, 32] and other power electronic devices [33, 34], etc. The VRC of the conventional network reinforcement solution serves as a benchmark, with which the costs of alternative solutions can be compared.

The rest of this paper is organized as follows: Section II presents a general VRC model based on equivalent impedance matrix; Section III presents five specific VRC models where each model considers a specific load current distribution; Section IV presents a case study; and Section V concludes the paper.

II. GENERAL VRC MODEL BASED ON EQUIVALENT IMPEDANCE MATRIX

A general VRC model is proposed in this section, accounting for the location-dependent impedance of different feeder sections and a generic distribution of demand currents along each phase of the feeder. The model considers uneven voltage drops along the three phases, based on substation-side voltages and currents under peak demand. Unless stated otherwise, all voltages and currents data used in this paper are monitored under the peak demand.

Denote x as the distance between the point concerned and the substation. Suppose the location-dependent impedance matrix is $Z(x)$. The distribution of demand currents along phase $\emptyset$ is denoted as $\dot{i}_{d\emptyset}(x)$.

The phase current at location x of phase $\emptyset$ is therefore given by

$$\dot{I}_{\emptyset}(x) = \int_{x}^{L} \dot{i}_{d\emptyset}(l)dl \quad \text{where } \emptyset \in \{a,b,c\} \quad (1)$$

where L is the length of the feeder.

The currents are monitored at the secondary side of the substation. They are given by

$$\dot{I}_{\emptyset}(0) = \int_{0}^{L} \dot{i}_{d\emptyset}(l)dl \quad \text{where } \emptyset \in \{a,b,c\} \quad (2)$$

The voltage drops at the end of the three phases are expressed as

$$\begin{bmatrix} \Delta\dot{V}_a \\ \Delta\dot{V}_b \\ \Delta\dot{V}_c \end{bmatrix} = \int_{0}^{L} Z(x) \begin{bmatrix} \dot{I}_a(x) \\ \dot{I}_b(x) \\ \dot{I}_c(x) \end{bmatrix} dx \quad (3)$$

Define the equivalent impedance matrix as the one that would lead to the same voltage drops at the feeder end, given the same substation-side currents. The equivalent impedance matrix is defined in the form of

$$Z_{eq} = \begin{bmatrix} Z_{eqa} & & \\ & Z_{eqb} & \\ & & Z_{eqc} \end{bmatrix} \quad (4)$$

Each diagonal element of $Z_{eq\emptyset}$ is a function of $\dot{I}_a(0)$, $\dot{I}_b(0)$, and $\dot{I}_c(0)$, implicitly incorporating the mutual inductance and the impact of the neutral current, as explained later in this section.

There is

$$\begin{bmatrix} Z_{eqa} & & \\ & Z_{eqb} & \\ & & Z_{eqc} \end{bmatrix} \begin{bmatrix} \dot{I}_a(0) \\ \dot{I}_b(0) \\ \dot{I}_c(0) \end{bmatrix} = \int_{0}^{L} Z(x) \begin{bmatrix} \dot{I}_a(x) \\ \dot{I}_b(x) \\ \dot{I}_c(x) \end{bmatrix} dx \quad (5)$$

It should be noted that $Z(x)$ on the right hand side of (5) considers both the transposed and non-transposed conditions of feeders. Rather than being a physical impedance, each equivalent impedance on the left hand side of (5) represents the relationship between the substation-side current of the phase in question and the terminal voltage drop of that phase. Such a relationship does not change when the load currents of the three phases grow by the same percentage each year, regardless of whether the three phases are transposed or not – this is proven in the Appendix. The invariability of this relationship enables the use of the equivalent impedance matrix.

The only three non-zero elements of the equivalent impedance matrix are given by

$$\begin{bmatrix} Z_{eqa} \\ Z_{eqb} \\ Z_{eqc} \end{bmatrix} = [\dot{I}_{\emptyset}(0)]^{-1} \cdot \int_{0}^{L} Z(x)[\int_{x}^{L} \begin{bmatrix} \dot{i}_{da}(l) \\ \dot{i}_{db}(l) \\ \dot{i}_{dc}(l) \end{bmatrix} dl]dx \quad (6)$$

where

$$[\dot{I}_{\emptyset}(0)]^{-1} = \begin{bmatrix} 1/\dot{I}_a(0) & & \\ & 1/\dot{I}_b(0) & \\ & & 1/\dot{I}_c(0) \end{bmatrix} \quad (7)$$

In this way, the equivalent impedance matrix Z_{eq} is obtained.

The mutual inductance and the impact of the neutral current are incorporated into $Z(x)$, resulting in non-zero off-diagonal elements of $Z(x)$. According to (6), the mutual inductance and the impact of the neutral current are therefore implicitly incorporated in the equivalent impedance matrix Z_{eq}: rather than reflecting them in the off-diagonal elements, Z_{eq} incorporates them in the diagonal elements $Z_{eq\emptyset}$ ($\emptyset \in \{a,b,c\}$) as the functions of $\dot{I}_a(0)$, $\dot{I}_b(0)$, and $\dot{I}_c(0)$. The network

representation of the equivalent impedance matrix Z_{eq} is presented in Fig. 1.

$Z_{eq\phi}=f_\phi(I_a(0), I_b(0), I_c(0))$

$Z_{eq\phi}$ is not a constant. Rather, it is a function of $I_a(0)$, $I_b(0)$, and $I_c(0)$, thereby incorporating the mutual inductance and the impact of the neutral line current.
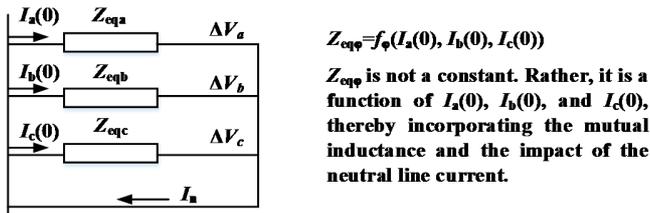
Fig. 1 Network representation of the equivalent impedance matrix Z_{eq}

It should be noted that $Z_{eq\phi}$ does not necessarily have a closed-form expression due to the integral nature, in which case numerical solutions should be sought for.

Suppose that the demand currents monitored at the substation grow by a percentage r each year, reflecting a long-term demand growth. By the end of the nth year, the feeder-end voltage drops are given by

$$\begin{bmatrix} \Delta \dot{V}_a \\ \Delta \dot{V}_b \\ \Delta \dot{V}_c \end{bmatrix} = \begin{bmatrix} Z_{eqa} & & \\ & Z_{eqb} & \\ & & Z_{eqc} \end{bmatrix} \begin{bmatrix} \dot{I}_a(0) \\ \dot{I}_b(0) \\ \dot{I}_c(0) \end{bmatrix} (1+r)^n \qquad (8)$$

where r denotes the annual growth rate of the demands.

According to (8), the use of the equivalent impedance matrix is the key, as it allows the voltage drops to be expressed as the functions of phase currents. Furthermore, the equivalent impedance matrix is invariant under demand growth, i.e. it is not a function of the annual demand growth rate r, as proven in the Appendix. This enables a straightforward non-iterative calculation of the VRC.

The number of years it takes the feeder-end voltage of phase ϕ to drop to the statutory lower limit is the solution to (8):

$$n_\phi = \frac{\log|\Delta \dot{V}_{\phi max}| - \log|Z_{eq\phi}| - \log|\dot{I}_\phi(0)|}{\log(1+r)} \qquad (9)$$

where $\phi \in \{a,b,c\}$; $\Delta \dot{V}_{\phi max}$ denotes the maximum allowed voltage drop; and r denotes the annual growth rate of the demands. Equation (9) shows that $Z_{eq\phi}$ is the key to the calculation of n_ϕ ($\phi \in \{a,b,c\}$).

A time horizon is defined as the number of years it takes for the feeder-end voltage to drop to the statutory lower limit. The time horizon of the feeder is the time horizon of the phase of which the terminal voltage first drops to the lower limit.

$$n = \min\{n_a, n_b, n_c\} \quad \text{where } \phi \in \{a,b,c\} \qquad (10)$$

The VRC is therefore given by

$$VRC = \frac{IC}{(1+d)^n} \qquad (11)$$

where IC and d denote the future reinforcement cost and the discount rate, respectively.

The general VRC model considers a range of factors:
1) The existence of different branch sections that have different impedance per unit length;
And 2) various customer allocation patterns and individual demand currents incorporated into a generic distribution of demand currents.

Theoretically, the demand current distribution can be infinitely accurate; but in reality, the exact location-dependent impedance matrix $Z(x)$ and the distribution of demand currents

$\dot{I}_{d\phi}(x)$ are unavailable due to the high cost to obtain them and the excessive computational burden of accounting for them on a utility scale. Even for an individual feeder, these data are not always available. This prompts the need to develop specific VRC models, which are derived by applying simplifications to the general VRC model. Therefore, the general VRC model introduced in this section serves as the basis for the specific VRC models introduced in the next section.

It should be noted that the VRC models, whether general or specific, are applicable to demand-dominated LV feeders with a low penetration of renewable generation.

III. SPECIFIC VRC MODELS BASED ON EQUIVALENT IMPEDANCE MATRIX

To overcome the challenges of data deficiency and scalability, approximations have to be made to the distributions of demand currents, thus leading to specific VRC models.

Kersting proposed a method to estimate voltage drops by assuming a constant load density in three typical geometric configurations, without considering three-phase imbalance [17]. These geometric configurations can be converted into the corresponding load current distributions along the feeder.

This paper makes a substantial enhancement by incorporating five demand current distributions into an equivalent impedance matrix for the VRC estimation under three-phase imbalance. The five distributions are the uniform, tail-dominated triangular, head-dominated triangular, trapezoid, and triangular-rectangular distributions.

Five specific VRC models are proposed based on two simplifications of the general VRC model:
1) A matrix of average impedance per unit length of the feeder is assumed, denoted as Z_{ave}.
2) Each specific VRC model corresponds to a particular distribution of the demand currents.

A. Uniform Distribution of Demand Currents

In this case, the demand current of each phase is distributed evenly along the feeder, as depicted in Fig. 2.
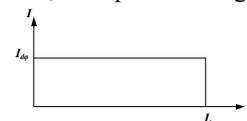

Fig. 2 Uniform distribution of demand currents on phase ϕ

The demand currents are presented as the functions of the distance l from the substation:

$$\begin{bmatrix} \dot{I}_{da}(l) \\ \dot{I}_{db}(l) \\ \dot{I}_{dc}(l) \end{bmatrix} = \begin{bmatrix} \dot{I}_{da} \\ \dot{I}_{db} \\ \dot{I}_{dc} \end{bmatrix} \qquad (12)$$

Substitute (12) and the average impedance matrix per unit length Z_{ave} into (6). The three non-zero elements of the equivalent impedance matrix form an equivalent impedance vector, given by

$$\begin{bmatrix} Z_{eqa} \\ Z_{eqb} \\ Z_{eqc} \end{bmatrix} = [\dot{I}_\emptyset(0)]^{-1} Z_{ave} \begin{bmatrix} \dot{I}_{da} \\ \dot{I}_{db} \\ \dot{I}_{dc} \end{bmatrix} \int_0^L (L-x)dx$$
$$= \frac{1}{2} L [\dot{I}_\emptyset(0)]^{-1} Z_{ave} \begin{bmatrix} \dot{I}_a(0) \\ \dot{I}_b(0) \\ \dot{I}_c(0) \end{bmatrix} \qquad (13)$$

Because $\dot{I}_\emptyset(0)$, L, and Z_{ave} are all known, a characteristic impedance vector is defined as:

$$[Z_{C\emptyset}] = \begin{bmatrix} Z_{Ca} \\ Z_{Cb} \\ Z_{Cc} \end{bmatrix} = L[\dot{I}_\emptyset(0)]^{-1} Z_{ave} \begin{bmatrix} \dot{I}_a(0) \\ \dot{I}_b(0) \\ \dot{I}_c(0) \end{bmatrix} \qquad (14)$$

Substitute (14) into (13). The equivalent impedance vector is given by

$$\begin{bmatrix} Z_{eqa} \\ Z_{eqb} \\ Z_{eqc} \end{bmatrix} = \frac{1}{2} [Z_{C\emptyset}] \qquad (15)$$

The number of years it takes for the feeder-end voltage of phase $\emptyset$ to drop to the statutory lower limit is calculated by substituting (15) into (9). The time horizon of the feeder is given by (10). The VRC is computed by (11).

B. Tail-Dominated Triangular Distribution of Demand Currents

In this case, the demand current of each phase increases linearly with the distance from the substation, as depicted in Fig. 3.
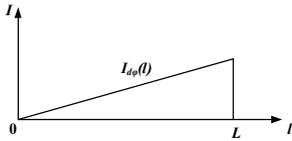

Fig. 3 Tail-dominated distribution of demand currents on phase $\emptyset$

The demand currents are given as the functions of the distance l from the substation:

$$\begin{bmatrix} \dot{I}_{da}(l) \\ \dot{I}_{db}(l) \\ \dot{I}_{dc}(l) \end{bmatrix} = l \begin{bmatrix} \dot{K}_a \\ \dot{K}_b \\ \dot{K}_c \end{bmatrix} \qquad (16)$$

The phase currents measured at the substation are given by

$$\begin{bmatrix} \dot{I}_a(0) \\ \dot{I}_b(0) \\ \dot{I}_c(0) \end{bmatrix} = \int_0^L \begin{bmatrix} \dot{I}_{da}(l) \\ \dot{I}_{db}(l) \\ \dot{I}_{dc}(l) \end{bmatrix} dl = \frac{1}{2} L^2 \begin{bmatrix} \dot{K}_a \\ \dot{K}_b \\ \dot{K}_c \end{bmatrix} \qquad (17)$$

There is

$$\begin{bmatrix} \dot{K}_a \\ \dot{K}_b \\ \dot{K}_c \end{bmatrix} = \frac{2}{L^2} \begin{bmatrix} \dot{I}_a(0) \\ \dot{I}_b(0) \\ \dot{I}_c(0) \end{bmatrix} \qquad (18)$$

Substitute (18) into (16) which is further substituted into (6). The three non-zero elements of the equivalent impedance matrix are given by

$$\begin{bmatrix} Z_{eqa} \\ Z_{eqb} \\ Z_{eqc} \end{bmatrix} = [\dot{I}_\emptyset(0)]^{-1} Z_{ave} \begin{bmatrix} \dot{K}_a \\ \dot{K}_b \\ \dot{K}_c \end{bmatrix} \int_0^L [\int_x^L l\, dl\,] dx =$$
$$\frac{2}{3} L [\dot{I}_\emptyset(0)]^{-1} Z_{ave} \begin{bmatrix} \dot{I}_a(0) \\ \dot{I}_b(0) \\ \dot{I}_c(0) \end{bmatrix} \qquad (19)$$

Substitute the characteristic impedance vector $[Z_{C\emptyset}]$ defined in (14) into (19). The three non-zero elements of the equivalent impedance matrix are given by

$$\begin{bmatrix} Z_{eqa} \\ Z_{eqb} \\ Z_{eqc} \end{bmatrix} = \frac{2}{3} [Z_{C\emptyset}] \qquad (20)$$

With the equivalent impedance matrix obtained, the VRC is then computed from (9) – (11).

C. Head-Dominated Triangular Distribution of Demand Currents

In this case, the demand current of each phase is decreasing linearly with the increase of the distance from the substation, as depicted in Fig. 4.
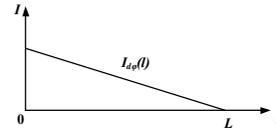

Fig. 4 Head-dominated distribution of demand currents on phase $\emptyset$

The demand currents are given as the functions of the distance l from the substation:

$$\begin{bmatrix} \dot{I}_{da}(l) \\ \dot{I}_{db}(l) \\ \dot{I}_{dc}(l) \end{bmatrix} = \begin{bmatrix} -\dfrac{\dot{a}}{L}l + \dot{a} \\ -\dfrac{\dot{b}}{L}l + \dot{b} \\ -\dfrac{\dot{c}}{L}l + \dot{c} \end{bmatrix} \qquad (21)$$

where $\dot{a} = \dot{I}_{da}(0)$, $\dot{b} = \dot{I}_{db}(0)$, and $\dot{c} = \dot{I}_{dc}(0)$.

The phase currents measured at the substation are given by

$$\begin{bmatrix} \dot{I}_a(0) \\ \dot{I}_b(0) \\ \dot{I}_c(0) \end{bmatrix} = \int_0^L \begin{bmatrix} \dot{I}_{da}(l) \\ \dot{I}_{db}(l) \\ \dot{I}_{dc}(l) \end{bmatrix} dl = \frac{1}{2} L \begin{bmatrix} \dot{a} \\ \dot{b} \\ \dot{c} \end{bmatrix} \qquad (22)$$

Therefore,

$$\begin{bmatrix} \dot{a} \\ \dot{b} \\ \dot{c} \end{bmatrix} = \frac{2}{L} \begin{bmatrix} \dot{I}_a(0) \\ \dot{I}_b(0) \\ \dot{I}_c(0) \end{bmatrix} \qquad (23)$$

Substitute (23) into (21) which is then substituted into (6). The three non-zero elements of the equivalent impedance matrix are given by

$$\begin{bmatrix} Z_{eqa} \\ Z_{eqb} \\ Z_{eqc} \end{bmatrix} = [\dot{I}_\emptyset(0)]^{-1} \int_0^L Z_{ave} [\int_x^L \begin{bmatrix} -\dfrac{\dot{a}}{L}l + \dot{a} \\ -\dfrac{\dot{b}}{L}l + \dot{b} \\ -\dfrac{\dot{c}}{L}l + \dot{c} \end{bmatrix} dl\,] dx =$$
$$\frac{1}{3} L [\dot{I}_\emptyset(0)]^{-1} Z_{ave} \begin{bmatrix} \dot{I}_a(0) \\ \dot{I}_b(0) \\ \dot{I}_c(0) \end{bmatrix} \qquad (24)$$

Substitute (14) into (24). Equation (24) is expressed as

$$\begin{bmatrix} Z_{eqa} \\ Z_{eqb} \\ Z_{eqc} \end{bmatrix} = \frac{1}{3} [Z_{C\emptyset}] \qquad (25)$$

With the equivalent impedance matrix obtained, the VRC is then computed by using (9) – (11).

D. Trapezoid Distribution of Demand Currents

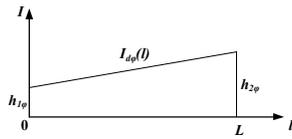In this case, the demand current of each phase is depicted in Fig. 5.

Fig. 5 Trapezoid distribution of demand currents on phase $\emptyset$

The demand currents are given by

$$
\begin{bmatrix} \dot{I}_{da}(l) \\ \dot{I}_{db}(l) \\ \dot{I}_{dc}(l) \end{bmatrix} = \begin{bmatrix} \dfrac{h_{2a} - h_{1a}}{L} l + h_{1a} \\ \dfrac{h_{2b} - h_{1b}}{L} l + h_{1b} \\ \dfrac{h_{2c} - h_{1c}}{L} l + h_{1c} \end{bmatrix} \tag{26}
$$

Where l is the distance from the substation; $h_{1\emptyset}$ and $h_{2\emptyset}$ ($\emptyset \in \{a, b, c\}$) are presented in Fig. 5.

The phase currents measured at the substation are given by

$$
\begin{bmatrix} \dot{I}_a(0) \\ \dot{I}_b(0) \\ \dot{I}_c(0) \end{bmatrix} = \frac{1}{2} L \begin{bmatrix} h_{1a} + h_{2a} \\ h_{1b} + h_{2b} \\ h_{1c} + h_{2c} \end{bmatrix} \tag{27}
$$

There is

$$
\begin{bmatrix} h_{2a} \\ h_{2b} \\ h_{2c} \end{bmatrix} = \begin{bmatrix} \dfrac{2}{L} \dot{I}_a(0) - h_{1a} \\ \dfrac{2}{L} \dot{I}_b(0) - h_{1b} \\ \dfrac{2}{L} \dot{I}_c(0) - h_{1c} \end{bmatrix} \tag{28}
$$

Where $0 \leq h_{1\emptyset} \leq \frac{2}{L} \dot{I}_\emptyset(0)$ for a demand-dominated feeder.

Substitute (28) into (26) which is further substituted into (6). The three non-zero elements of the equivalent impedance matrix are given by

$$
\begin{bmatrix} Z_{eqa} \\ Z_{eqb} \\ Z_{eqc} \end{bmatrix} = [\dot{I}_\emptyset(0)]^{-1} \int_0^L Z_{ave} [\int_x^L \begin{bmatrix} -\frac{\dot{a}}{L} l + \dot{a} \\ -\frac{\dot{b}}{L} l + \dot{b} \\ -\frac{\dot{c}}{L} l + \dot{c} \end{bmatrix} dl] dx =
$$

$$
L[\dot{I}_\emptyset(0)]^{-1} Z_{ave} \begin{bmatrix} \frac{2}{3} \dot{I}_a(0) - \frac{1}{6} L h_{1a} \\ \frac{2}{3} \dot{I}_b(0) - \frac{1}{6} L h_{1b} \\ \frac{2}{3} \dot{I}_c(0) - \frac{1}{6} L h_{1c} \end{bmatrix} \tag{29}
$$

Substitute (14) into (29). The three non-zero elements of the equivalent impedance matrix are expressed as

$$
\begin{bmatrix} Z_{eqa} \\ Z_{eqb} \\ Z_{eqc} \end{bmatrix} = \frac{2}{3} [Z_{C\emptyset}] - \frac{1}{6} L^2 [\dot{I}_\emptyset(0)]^{-1} Z_{ave} \begin{bmatrix} h_{1a} \\ h_{1b} \\ h_{1c} \end{bmatrix} \tag{30}
$$

Equation (30) demonstrates that, for each phase, only one variable among $h_{1\emptyset}$ and $h_{2\emptyset}$ is independent.

The uniform, tail-dominated triangle, and head-dominated triangle distributions are the special cases of the trapezoid distribution, where $h_{1\emptyset} = h_{2\emptyset}$, $h_{1\emptyset} = 0$, and $h_{2\emptyset} = 0$, respectively.

Let $h_{1\emptyset} = \frac{K_\emptyset}{L} \dot{I}_\emptyset(0)$, where $K_\emptyset$ is the K factor ($0 \leq K_\emptyset \leq 2$). Equation (30) is transformed into

$$
\begin{bmatrix} Z_{eqa} \\ Z_{eqb} \\ Z_{eqc} \end{bmatrix} = \frac{2}{3} [Z_{C\emptyset}] - \frac{1}{6} L [\dot{I}_\emptyset(0)]^{-1} Z_{ave} \begin{bmatrix} K_a \dot{I}_a(0) \\ K_b \dot{I}_b(0) \\ K_c \dot{I}_c(0) \end{bmatrix} \tag{31}
$$

$K_\emptyset$ is the parameter that determines the shape of the load current distribution for phase $\emptyset$. A greater $K_\emptyset$ means that the distribution is more skewed towards the substation side. The uniform, tail-dominated triangle, and head-dominated triangle distributions correspond to $K_\emptyset = 1$, $K_\emptyset = 0$, and $K_\emptyset = 2$, respectively.

Given a lack of smart metering data, equation (30) can be simplified by assuming that the K factors are the same for the three phases:

$$
h_{1\emptyset} = \frac{K}{L} \dot{I}_\emptyset(0) \tag{32}
$$

where $0 \leq K \leq 2$. This is equivalent to assuming that the load current distributions of the three phases follow a similar pattern.

Therefore, the three non-zero elements of the equivalent impedance matrix are expressed as

$$
\begin{bmatrix} Z_{eqa} \\ Z_{eqb} \\ Z_{eqc} \end{bmatrix} = \frac{4 - K}{6} [Z_{C\emptyset}] \tag{33}
$$

Where $[Z_{C\emptyset}]$ is defined in (14).

With the equivalent impedance matrix obtained, the VRC is then computed from (9) – (11).

E. Triangular-Rectangular Distribution of Demand Currents

In this case, the triangular-rectangular (TR) distribution of demand currents on phase $\emptyset$ is depicted in Fig. 6.
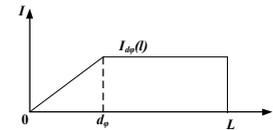

Fig. 6 Triangular-rectangular distribution of demand currents on phase $\emptyset$

The demand currents on phase $\emptyset$ are given by

$$
\dot{I}_{d\emptyset}(l) = \begin{cases} \dfrac{2 I_\emptyset(0)}{d_\emptyset (2L - d_\emptyset)} l & \text{when } 0 \leq l < d_\emptyset \\ \dfrac{2 I_\emptyset(0)}{2L - d_\emptyset} & \text{when } d_\emptyset \leq l \leq L \end{cases} \tag{34}
$$

Where $d_\emptyset$ ($\emptyset \in \{a, b, c\}$) is defined in Fig. 6 as the border point between the triangle and the rectangle. There is $0 \leq d_\emptyset \leq L$.

The three non-zero elements of the equivalent impedance matrix are derived following the same process as in the previous section.

$$
\begin{bmatrix} Z_{eqa} \\ Z_{eqb} \\ Z_{eqc} \end{bmatrix} = [\dot{I}_\emptyset(0)]^{-1} Z_{ave} \begin{bmatrix} \dot{I}_a(0) \cdot \dfrac{3L^2 - d_a^2}{3(2L - d_a)} \\ \dot{I}_b(0) \cdot \dfrac{3L^2 - d_b^2}{3(2L - d_b)} \\ \dot{I}_c(0) \cdot \dfrac{3L^2 - d_c^2}{3(2L - d_c)} \end{bmatrix} \tag{35}
$$

The uniform and tail-dominated distributions are the special cases of the TR distribution, where $d_\emptyset = 0$ and $d_\emptyset = L$, respectively.

Let $d_\emptyset = \beta_\emptyset L$, where $\beta_\emptyset$ is the beta factor ($0 \leq \beta_\emptyset \leq 1$). Equation (35) is transformed into

$$
\begin{bmatrix} Z_{eqa} \\ Z_{eqb} \\ Z_{eqc} \end{bmatrix} = L [\dot{I}_\emptyset(0)]^{-1} Z_{ave} \begin{bmatrix} \dot{I}_a(0) \cdot \dfrac{3 - \beta_a^2}{3(2 - \beta_a)} \\ \dot{I}_b(0) \cdot \dfrac{3 - \beta_b^2}{3(2 - \beta_b)} \\ \dot{I}_c(0) \cdot \dfrac{3 - \beta_c^2}{3(2 - \beta_c)} \end{bmatrix} \tag{36}
$$

$\beta_\emptyset$ is the parameter that determines the shape of the load current distribution for phase $\emptyset$. A greater $\beta_\emptyset$ means that the distribution is more skewed towards the feeder end. The uniform and tail-dominated distributions correspond to $\beta_\emptyset = 0$ and $\beta_\emptyset = 1$, respectively.

Given a lack of smart metering data, equation (35) can be simplified by assuming that the beta factors are the same for the three phases:

$$d_\emptyset = \beta L \qquad (37)$$

Where $0 \le \beta \le 1$. This is equivalent to assuming that the load current distributions of the three phases follow a similar pattern.

Therefore, the three non-zero elements of the equivalent impedance matrix are given by

$$\begin{bmatrix} Z_{eqa} \\ Z_{eqb} \\ Z_{eqc} \end{bmatrix} = \frac{3 - \beta^2}{3(2 - \beta)} [Z_{C\emptyset}] \qquad (38)$$

Where $[Z_{C\emptyset}]$ is defined in (14).

With the equivalent impedance matrix obtained, the VRC is then computed from (9) – (11).

IV. CASE STUDY

The methodology is applied to an individual feeder, based on the substation-side three-phase currents and voltages data. The input data for the base case are presented in Table I.

TABLE I: GENERAL INPUT DATA

Variable	Value	Variable	Value
$I_a(0)$	72A	$V_a(0)$	245V [4]
$I_b(0)$	69A	$V_b(0)$	245V
$I_c(0)$	58A	$V_c(0)$	245V
L	1500m	r	1.9% [35]
d	6.9% [35]	Power factor	0.95 [36]
Z+	0.868+j0.092Ω/km [37]	Z0	0.760+j0.092Ω/km [37]
IC*	£5,800 [8]		

*Future reinforcement cost

Suppose that the demand currents of the three phases follow a trapezoid distribution with the same K factor (uniform, tail-dominated triangular, and head-dominated triangular distributions are the special cases of the trapezoid distribution). The VRCs are computed under a range of K factors, as depicted in Fig. 7.
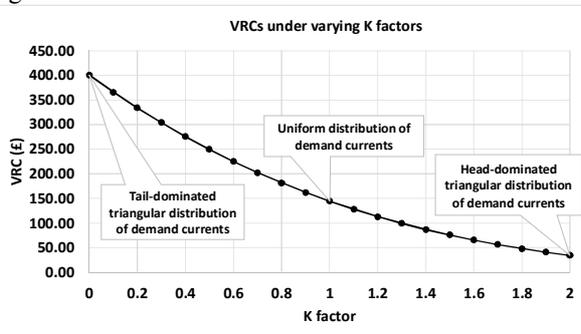

Fig. 7 VRCs under varying K factors

Fig. 7 shows that the VRC decreases with the increase of the K factor, because an increasing K factor causes the demand current distributions to be skewed towards the substation side,

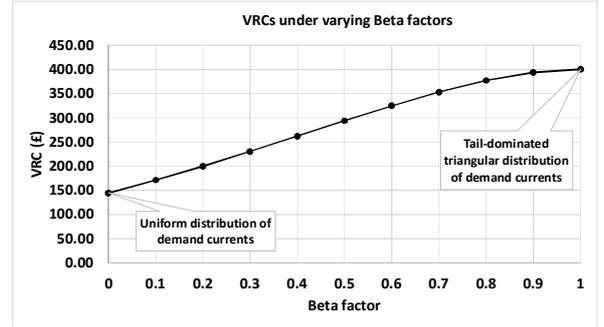thus reducing the voltage drops of the three phases and leading to a decrease of the VRC.

Fig. 8 VRCs under varying β factors

Suppose that the demand currents of the three phases follow a triangular-rectangular distribution with the same β factor, where uniform and tail-dominated triangular distributions are the special cases. The VRCs are computed under a range of β factors, as depicted in Fig. 8.

Fig. 8 shows that the VRC increases with β, because an increasing β corresponds to an increasing skewness of the demand current distributions towards the feeder terminal, thus increasing the voltage drops of the three phases and the VRC.

A. The Impact of Voltage Imbalance on VRCs

According to Table I, the substation-side phase voltages $V_\emptyset(0)$ are assumed to be balanced at 245V for the base case. In this section, the impact of voltage imbalance on the VRC is investigated by considering a range of $V_a(0)$, whilst maintaining other input variables constant. Suppose that the demand current distributions of the three phases follow a trapezoid distribution with the same K factor. The VRCs are computed under a range of $V_a(0)$ deviations from the balanced value, as depicted in Fig. 9.

Fig. 9 shows that the VRC is highly sensitive to voltage imbalance. Given any K factor, the VRC first decreases with the increase of $V_a(0)$ when the percentage deviation is less equal to 0%, i.e. when $V_a(0) \le 245V$; then, the VRC remains constant when the percentage deviation is positive, i.e. when $V_a(0) > 245V$. This is because:

1) When $V_a(0) \le 245V$, phase a is the phase of which the terminal voltage will first drop to the statutory lower limit under long-term demand growth – phase a determines the voltage spare room of the feeder and the VRC. An increasing $V_a(0)$ within the range enlarges the voltage spare room and reduces the VRC.

2) When $V_a(0) > 245V$, phases b and c restrain the voltage spare room. An increasing $V_a(0)$ does not enlarge the voltage spare room, hence not affecting the VRC.
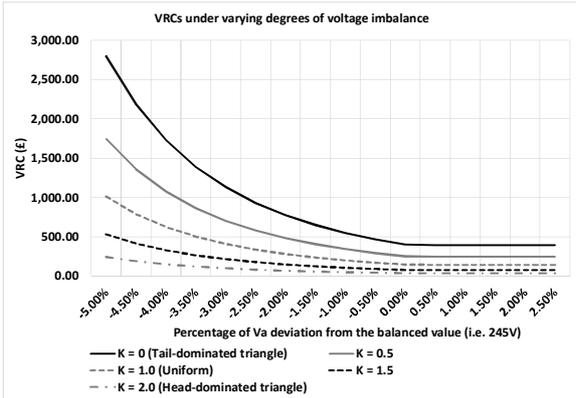
Fig. 9 VRCs under varying degrees of voltage imbalance

B. The Impact of Current Imbalance on VRCs

Suppose that $I_b(0) = I_c(0) = 72A$. All other data are the same as in Table I. The impact of current imbalance on the VRC is investigated by considering $I_a(0)$ within a percentage deviation range of [-20%, 20%], i.e. $I_a(0) \in [57.6A, 86.4A]$. Suppose that the demand currents of the three phases follow the trapezoid distribution with the same K factor.

The VRC results are depicted in Fig. 10. Given any K factor, the VRC reaches its minimum when the currents are balanced, corresponding to a 0% deviation of $I_a(0)$ from the balanced value. This is because:

1) When $I_a(0)$ is less than the currents of the other two phases (the percentage of deviation is negative), a decreasing $I_a(0)$ causes a relatively slow decrease of the terminal voltages for phases b and c due to the mutually coupling nature reflected by the impedance matrix Z_{ave}, leading to a relatively slow increase of the VRC.

2) When $I_a(0)$ is greater than the currents of the other two phases (the percentage of deviation is positive), an increasing $I_a(0)$ causes a relatively fast decrease of the terminal voltage for phase a, causing a relatively fast increase of the VRC.

The words 'fast' and 'slow' are relative between the above two cases. The results demonstrate that the VRC is more sensitive to voltage imbalance than to current imbalance.

It should be noted that the results are true when only one input variable is changed, whilst all other input variables remain constant.
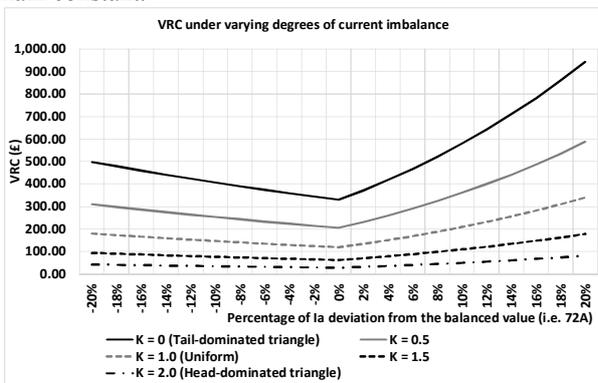

Fig. 10 VRCs under varying degrees of current imbalance

C. The Impact of K-Factor Imbalance on VRCs

In this section, $I_a(0) = I_b(0) = I_c(0) = 72A$. Other data are presented in Table I. Phases b and c have the same K factor, $K_b = K_c$. The impact of the K factor on VRCs is investigated by considering a range of $K_a \in [0.0, 2.0]$, whilst maintaining other input variables constant. The VRC results are plotted in Fig. 11.

The VRC reaches its minimum when $K_a = K_b = K_c$, i.e. when the load current distributions of the three phases have the same K factor, given that $I_a(0) = I_b(0) = I_c(0)$ and $V_a(0) = V_b(0) = V_c(0)$. This is because:

1) When $K_a = K_b = K_c$, the three phases are balanced, with a phase current of 72A.

2) When $K_a \neq K_b = K_c$, at least one phase has a current greater than 72A, resulting in a lower feeder-end voltage of that phase and a greater VRC than that in the balanced case.
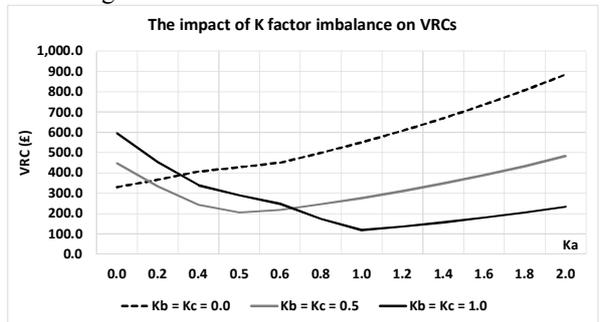

Fig. 11 VRCs under imbalanced K factors

D. The Impact of Beta-Factor Imbalance on VRCs

In this section, $I_a(0) = I_b(0) = I_c(0) = 72A$. Other data are the same as in Table I. Phases b and c have the same β factor, $\beta_b = \beta_c$. The impact of the K factor on VRCs is investigated by considering a range of $\beta_a \in [0.0, 1.0]$, whilst maintaining other input variables constant. The VRC results are plotted in Fig. 12.

The VRC reaches its minimum when $\beta_a = \beta_b = \beta_c$, i.e. when the load current distributions of the three phases have the same β factor, given that $I_a(0) = I_b(0) = I_c(0)$ and $V_a(0) = V_b(0) = V_c(0)$. The reason is similar to that in the previous section:

1) When $\beta_a = \beta_b = \beta_c$, the three phases are balanced, where the phase current is 72A.

2) When $\beta_a \neq \beta_b = \beta_c$, at least one phase has a current greater than 72A, resulting in a lower feeder-end voltage of that phase and a greater VRC than that in the balanced case.
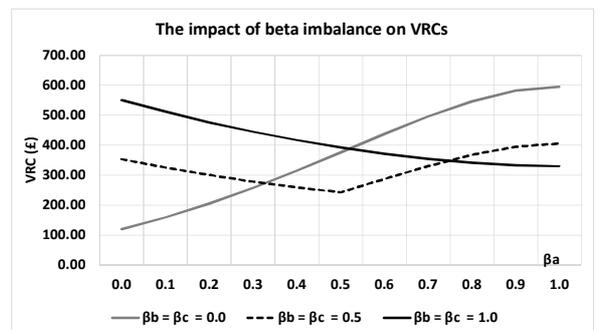

Fig. 12 VRCs under imbalanced β factors

Sections IV. C – D prove that the balanced condition corresponds to the minimum VRC; if any single variable

deviates from the balanced condition whilst other input variables remain unchanged, the VRC will increase.

E. Discussions

The conclusions in Sections IV. A – D are true under the condition that the average impedance matrix per unit length of the feeder is based on the approximate line model introduced in [17]. The approximate line model is applicable when the negative sequence impedance is unknown, which is normally the case in reality.

The proposed methodology applies to demand-dominated LV networks with a low penetration of renewable energy. Future work will extend the methodology to consider a high penetration of renewable energy.

The method has the prospect to be scaled up to a utility level due to: 1) its non-iterative nature as opposed to power-flow-based methods; 2) the ability to account for a variety of load current distributions; and 3) the suitability where the level of information is insufficient to support feeder-by-feeder power flow studies. The next stage of the research will be applying the method to a utility scale with millions of feeders.

V. CONCLUSIONS

This paper proposes a novel scalable methodology for voltage-driven reinforcement cost (VRC) estimations where the level of information required for an accurate three-phase power flow study is not available. The methodology consists of a novel general VRC model and five novel specific VRC models. The five models incorporate five typical load current distributions (i.e. the uniform, head-dominated triangular, tail-dominated triangular, trapezoid, and triangular-rectangular distributions) into an invariant equivalent impedance matrix for a straightforward non-iterative estimation of the VRC. The following conclusions are drawn from the case study:

1) The VRC decreases with the increase of the parameter K for the trapezoid distribution, given other conditions the same.

2) The VRC increases with the beta factor of the triangular-rectangular distribution, given other conditions the same.

3) The VRC is highly sensitive to voltage imbalance. If two phases have the same voltage magnitude at the substation side, the VRC reaches the minimum when the third phase has a voltage of which the magnitude is no less than that of the other two phases, given other conditions the same and that the phase angles are 120° apart from each other.

4) If the three phases are originally balanced, the change of any single variable will result in an increase of the VRC, given that all other input variables remain unchanged and that the average impedance matrix is based on the approximate line model introduced in [17].

The VRC models demonstrate suitability for cases with severe data deficiency and the prospect to be scaled up to a utility level with millions of feeders.

REFERENCES

[1] L. Yun and P. A. Crossley, "Voltage balancing in low-voltage radial feeders using scott transformers," *Generation, Transmission & Distribution, IET,* vol. 8, pp. 1489-1498, 2014.

[2] N. C. Woolley and J. V. Milanovic, "Statistical Estimation of the Source and Level of Voltage Unbalance in Distribution Networks," *Power Delivery, IEEE Transactions on,* vol. 27, pp. 1450-1460, 2012.

[3] M. W. Siti, D. V. Nicolae, A. A. Jimoh, and A. Ukil, "Reconfiguration and Load Balancing in the LV and MV Distribution Networks for Optimal Performance," *Power Delivery, IEEE Transactions on,* vol. 22, pp. 2534-2540, 2007.

[4] K. Ma, F. Li, and R. Aggarwal, "Quantification of Additional Reinforcement Cost Driven by Voltage Constraint Under Three-Phase Imbalance," *Power Systems, IEEE Transactions on,* vol. PP, pp. 1-9, 2016.

[5] A. Navarro, T. Gozel, L.F. Ochoa, R. Shaw, and D. Randles, "Data analysis of LV networks: Determination of key parameters from one year of monitoring over hundreds of UK LV feeders," presented at the 23rd International Conference on Electricity Distribution CIRED 2015, Lyon, 2015.

[6] L. F. O. A. Navarro, R. Shaw, D. Randles, "Reconstruction of low voltage networks: From GIS data To power flow models," presented at the 23rd International Conference on Electricity Distribution CIRED 2015, Lyon, 2015.

[7] (2013). *RIIO-ED1 HV and LV network investment analysis.* Available: http://www.spenergynetworks.co.uk/userfiles/file/201303_A2_4_TNEI_HV_LV_network_investment_analysis.pdf

[8] Y. Zhang, F. Li, Z. Hu, and G. Shaddick, "Quantification of low voltage network reinforcement costs: A statistical approach," *Power Systems, IEEE Transactions on,* vol. 28, pp. 810-818, 2013.

[9] A. M. Cossi, R. Romero, and J. Mantovani, "Planning and Projects of Secondary Electric Power Distribution Systems," *Power Systems, IEEE Transactions on,* vol. 24, pp. 1599-1608, 2009.

[10] A. Navarro and H. Rudnick, "Large-Scale Distribution Planning Part I: Simultaneous Network and Transformer Optimization," *Power Systems, IEEE Transactions on,* vol. 24, pp. 744-751, 2009.

[11] T. Sugita, D. Iioka, Y. Yokomizu, T. Matsumura, N. Hatakeyama, T. Kuriyama, and T. Ootaki, "Low-voltage distribution network planning taking account of power loss cost in genetic algorithms," in *Future Power Systems, 2005 International Conference on,* 2005, pp. 5-10.

[12] I. Ziari, G. Ledwich, A. Ghosh, and G. Platt, "Optimal distribution network reinforcement considering load growth, line loss, and reliability," *Power Systems, IEEE Transactions on,* vol. 28, pp. 587-597, 2013.

[13] T. Asakura, T. Genji, T. Yura, N. Hayashi, and Y. Fukuyama, "Long-term distribution network expansion planning by network reconfiguration and generation of construction plans," *Power Systems, IEEE Transactions on,* vol. 18, pp. 1196-1204, 2003.

[14] B. Zeng, J. Zhang, X. Yang, J. Wang, J. Dong, and Y. Zhang, "Integrated Planning for Transition to Low-Carbon Distribution System With Renewable Energy Generation and Demand Response," *Power Systems, IEEE Transactions on,* vol. 29, pp. 1153-1165, 2014.

[15] S. Favuzza, G. Graditi, M. G. Ippolito, and E. R. Sanseverino, "Optimal Electrical Distribution Systems Reinforcement Planning Using Gas Micro Turbines by Dynamic Ant Colony Search Algorithm," *Power Systems, IEEE Transactions on,* vol. 22, pp. 580-587, 2007.

[16] Z. Hu and F. Li, "Cost-Benefit Analyses of Active Distribution Network Management, Part II: Investment Reduction Analysis," *IEEE Transactions on Smart Grid,* vol. 3, pp. 1075-1081, 2012.

[17] W. H. Kersting, *Distribution System Modeling and Analysis, Third Edition,* 3 ed.: CRC Press, 2012.

[18] S. Yan, S. C.Tan, C. K. Lee, B. Chaudhuri, and S. Hui, "Electric Springs for Reducing Power Imbalance in Three-Phase Power Systems," *Power Electronics, IEEE Transactions on,* vol. 30, pp. 3601-3609, 2014.

[19] L. F. Ochoa, R. M. Ciric, A. Padilha-Feltrin, and G. P. Harrison, "Evaluation of distribution system losses due to load unbalance," presented at the Power Systems Computation Conference, Liege, 2005.

[20] E. Carpaneto, G. Chicco, and J. S. Akilimali, "Loss Partitioning and Loss Allocation in Three-Phase Radial Distribution Systems With Distributed Generation," *Power Systems, IEEE Transactions on,* vol. 23, pp. 1039-1049, 2008.

[21] V. Borozan, D. Rajicic, and R. Ackovski, "Minimum loss reconfiguration of unbalanced distribution networks," *Power Delivery, IEEE Transactions on,* vol. 12, pp. 435-442, 1997.

[22] A. Jalilian and R. Roshanfekr, "Analysis of Three-phase Induction Motor Performance under Different Voltage Unbalance Conditions Using Simulation and Experimental Results," *Electric Power Components and Systems,* vol. 37, pp. 300-319, 2009/02/23 2009.

[23] C. Yung, "Stopping a Costly Leak: The Effects of Unbalanced Voltage on the Life and Efficiency of Three-Phase Electric Motors," *Energy Matters,* vol. 30, 2005.

[24] A. Siddique, G. S. Yadava, and B. Singh, "Effects of voltage unbalance on induction motors," in *Electrical Insulation, 2004. Conference Record of the 2004 IEEE International Symposium on*, 2004, pp. 26-29.

[25] J. Zhu, M. Y. Chow, and F. Zhang, "Phase balancing using mixed-integer programming [distribution feeders]," *Power Systems, IEEE Transactions on,* vol. 13, pp. 1487-1492, 1998.

[26] J. Zhu, G. Bilbro, and M.-Y. Chow, "Phase balancing using simulated annealing," *Power Systems, IEEE Transactions on,* vol. 14, pp. 1508-1513, 1999.

[27] K. Ma, R. Li, and F. Li, "Quantification of Additional Asset Reinforcement Cost From 3-Phase Imbalance," *IEEE Transactions on Power Systems,* vol. In press, 2015.

[28] C. Zhao, C. Gu, F. Li, and M. Dale, "Understanding LV network voltage distribution- UK smart grid demonstration experience," in *Innovative Smart Grid Technologies Conference (ISGT), 2015 IEEE Power & Energy Society*, 2015, pp. 1-5.

[29] K. H. Chua, J. Wong, Y. S. Lim, P. Taylor, E. Morris, and S. Morris, "Mitigation of Voltage Unbalance in Low Voltage Distribution Network with High Level of Photovoltaic System," *Energy Procedia,* vol. 12, pp. 495-501, 2011.

[30] K. H. Chua, Y. S. Lim, P. Taylor, S. Morris, and J. Wong, "Energy Storage System for Mitigating Voltage Unbalance on Low-Voltage Networks With Photovoltaic Systems," *IEEE Transactions on Power Delivery,* vol. 27, pp. 1783-1790, 2012.

[31] A. Campos, G. Joos, P. D. Ziogas, and J. F. Lindsay, "Analysis and design of a series voltage unbalance compensator based on a three-phase VSI operating with unbalanced switching functions," *IEEE Transactions on Power Electronics,* vol. 9, pp. 269-274, 1994.

[32] C. Jen-Hung, L. Wei-Jen, and C. Mo-Shing, "Using a static VAr compensator to balance a distribution system," in *Industry Applications Conference, 1996. Thirty-First IAS Annual Meeting, IAS '96., Conference Record of the 1996 IEEE*, 1996, pp. 2321-2326 vol.4.

[33] V. B. Bhavaraju and P. N. Enjeti, "An active line conditioner to balance voltages in a three-phase system," *IEEE Transactions on Industry Applications,* vol. 32, pp. 287-292, 1996.

[34] D. A. Rendusara, A. V. Jouanne, P. N. Enjeti, and D. A. Paice, "Design considerations for 12-pulse diode rectifier systems operating under voltage unbalance and pre-existing voltage distortion with some corrective measures," *IEEE Transactions on Industry Applications,* vol. 32, pp. 1293-1303, 1996.

[35] F. Li and D. L. Tolley, "Long-Run Incremental Cost Pricing Based on Unused Capacity," *Power Systems, IEEE Transactions on,* vol. 22, pp. 1683-1689, 2007.

[36] A. J. Collin, G. Tsagarakis, A. E. Kiprakis, and S. McLaughlin, "Development of Low-Voltage Load Models for the Residential Load Sector," *Power Systems, IEEE Transactions on,* vol. 29, pp. 2180-2188, 2014.

[37] (2015, 08 Mar 2016). *Distribution Test Feeders.* Available: http://ewh.ieee.org/soc/pes/dsacom/testfeeders/index.html

Appendix: Proof of Invariability of the Equivalent Impedance Matrix under Demand Growth

The invariability of the equivalent impedance matrix used in the VRC models is proven in this section: after N years' demand growth, the demand current and phase current are given by

$$\dot{I}'_{d\emptyset}(l) = \dot{I}_{d\emptyset}(l)(1+r)^N \qquad (39)$$

$$\dot{I}'_{\emptyset}(l) = \dot{I}_{\emptyset}(l)(1+r)^N \qquad (40)$$

where l and r denote the distance from the substation and the annual demand growth rate, respectively.

The three non-zero elements of the equivalent impedance matrix are given by

$$\begin{bmatrix} Z'_{eqa} \\ Z'_{eqb} \\ Z'_{eqc} \end{bmatrix} = \frac{1}{(1+r)^N} [I_{\emptyset}(0)]^{-1} \cdot \int_0^L Z(x)[(1+r)^N \int_x^L \begin{bmatrix} \dot{I}_{da}(l) \\ \dot{I}_{db}(l) \\ \dot{I}_{dc}(l) \end{bmatrix} dl]dx \qquad (41)$$

Equation (41) leads to

$$\begin{bmatrix} Z'_{eqa} \\ Z'_{eqb} \\ Z'_{eqc} \end{bmatrix} = [I_{\emptyset}(0)]^{-1} \cdot \int_0^L Z(x)[\int_x^L \begin{bmatrix} \dot{I}_{da}(l) \\ \dot{I}_{db}(l) \\ \dot{I}_{dc}(l) \end{bmatrix} dl]dx = \begin{bmatrix} Z_{eqa} \\ Z_{eqb} \\ Z_{eqc} \end{bmatrix} \qquad (42)$$

Therefore, the equivalent impedance matrix is proved to be invariant under demand growth, i.e. it is not a function of the annual demand growth rate r. This is a very important feature as it allows the VRC to be calculated in a straightforward non-iterative way.